PERGAMON

International Journal of Solids and Structures 40 (2003) 5669–5688

INTERNATIONAL JOURNAL OF SOLIDS and STRUCTURES

www.elsevier.com/locate/ijsolstr

Finite polycrystalline elastoplasticity and damage: multiscale kinematics

J.D. Clayton [a,*], D.L. McDowell [b]

[a] *Impact Physics Branch, Army Research Laboratory, AMSRL-WM-TD, Aberdeen Proving Ground, MD 21005-5069, USA*
[b] *G.W.W. School of Mechanical Engineering, Georgia Institute of Technology, Atlanta, GA 30332-0405, USA*

Received 10 March 2003; received in revised form 2 June 2003

Abstract

A physically realistic macroscopic decomposition of the deformation gradient for metallic polycrystals should explicitly account for all relevant sub-macroscopic kinematic processes, including lattice deformation, plastic flow, and evolution of damage, that significantly contribute to the homogenized deformation at the macroscale. The present work suggests such a decomposition, based on principles of volume averaging and focusing upon elastoplasticity and a variety of damage modes including intergranular fracture, void growth and coalescence, and shear discontinuities. This decomposition, of hybrid additive–multiplicative form, captures precisely the kinematics of arbitrarily anisotropic damage and also offers insight into mesoscopic distributions of residual elastic lattice strain attributed to heterogeneity of local deformation occurring at both intergranular and intragranular scales.

Keywords: Damage criteria; Elastoplasticity; Homogenization; Kinematics; Micromechanics

1. Introduction

The *multiplicative* decomposition of the deformation gradient into elastic and plastic parts has been used to characterize sub-grain scale elastoplastic deformation in continuously distributed dislocation theory (Bilby et al., 1957; Kröner, 1960), single crystal deformation in classical crystal plasticity theory (Rice, 1971; Teodosiu and Sidoroff, 1976; Asaro, 1983; Peirce et al., 1983), and polycrystalline deformation in macroscopic plasticity models (Lee and Liu, 1967; Lee, 1969; Bammann and Johnson, 1987; Maugin, 1994; Scheidler and Wright, 2001). Models have also been proposed that incorporate explicit representations of damage in the multiplicative decomposition (Bammann and Aifantis, 1989; Park and Voyiadjis, 1998; Voyiadjis and Park, 1999). Isotropic damage is implicitly included in the plastic deformation gradient of many macroscopic formulations of porous inelasticity (cf. Nemat-Nasser et al., 1981; Marin and McDowell, 1996). Throughout the present work we denote by "damage" any deformation modes that render

* Corresponding author. Tel.: +1-410-306-0975; fax: +1-410-306-0783.
E-mail address: jclayton@arl.army.mil (J.D. Clayton).

0020-7683/$ - see front matter © 2003 Published by Elsevier Ltd.
doi:10.1016/S0020-7683(03)00317-2

the displacement field discontinuous, causing separation or (effectively) infinite strain in the material when observed at the micron scale. Thus, our definition of damage encompasses crack initiation and propagation, void initiation and growth, and localized shear flow wherein a finite tangential displacement jump (i.e., effectively infinite shear strain or a so-called "strong discontinuity") occurs across the shear band. Large but finite plastic strains, however, are excluded from this definition, since the glide of discrete dislocations (i.e., lattice displacement discontinuities) is typically resolved only at sub-micron scales of observation. Also excluded from "damage" are so-called "weak discontinuities" wherein displacements and deformation gradients are continuous everywhere, but velocity gradients and/or higher-order displacement gradients may not be so (cf. Rice, 1976; Duszek and Perzyna, 1991).

Additive decompositions for the deformation gradient have also been proposed for modeling elastoplasticity (Nemat-Nasser, 1979; Pantelides, 1994; Davison, 1995; Shen, 1998), phase transitions (Petryk, 1998), shear discontinuities (Armero and Garikipati, 1996; Pęcherski, 1998), and distributed microcracks (Zhou and Zhai, 1999). Additive decompositions of the spatial deformation rate tensor into elastic and inelastic parts are also popular in macroscopic numerical implementations (cf. Nemat-Nasser and Li, 1994). Recent micromorphic models of damage (Fu et al., 1998; Stumpf and Saczuk, 2000, 2001; Saczuk, 2001) have incorporated an additive decomposition of a covariant derivative defining the total deformation gradient on differentiable manifolds in Finsler space (cf. Rund, 1959), leading to an additive representation of macro- and microdeformations.

Previous models have often used a restricted form of the damage term in the decomposition of the total deformation gradient. A common element of macroscopic porous inelasticity is a purely isotropic damage deformation component defined completely in terms of the void volume fraction (Bammann and Aifantis, 1989; Bammann et al., 1993; Marin and McDowell, 1996). Voyiadjis and Park (1999) employed a *fictitious* deformation gradient term to model anisotropic damage; however, in their model this damage term is required to be symmetric in order to facilitate calculation of the symmetric effective stress. Others (Murakami, 1983, 1988, 1990; Fu et al., 1998; Steinmann and Carol, 1998) have used an area transformation rule (i.e., Nanson's formula) to calculate an effective stress resulting from a mapping between the current configuration and a fictitious, mechanically equivalent undamaged configuration. Brünig (2002) used a multiplicative decomposition of metric tensors to obtain multiple effective, fictitious undamaged configurations. These fictitious damage mapping approaches, while quite valid for characterizing material integrity and effective stresses, are neither suited nor intended for modeling the kinematic contributions of general damage entities.

In contrast, the current work suggests a kinematic decomposition incorporating explicit damage terms in the actual deformation gradient capable of describing general anisotropic damage. No restrictions (in terms of symmetry or isotropy) are imposed on the form of the damage terms in the deformation gradient. Thus, in contrast to many of the above-mentioned isotropic representations technically limited to uniform distributions of spherical voids, our approach permits accurate resolution of the kinematic contributions of damage entities of arbitrary geometry, such as non-uniform void clusters (e.g., coalescence of elliptical voids) and cracks or shear discontinuities of arbitrary orientation. More specifically, a hybrid additive–multiplicative decomposition is proposed, applicable for describing the collective deformation of multiple grains and assorted damage entities contained within a polycrystalline body. Components of the decomposition are determined via principles of volume averaging, with the formulation herein describing the physics of finite elastoplasticity coupled with one or more distinct damage modes. The interested reader is also referred to a previous multiscale formulation by the current authors (Clayton and McDowell, 2003) limited to *continuous* finite elastoplasticity and effectively extended herein to describe the homogenized kinematics of anisotropic damage.

The following notation is used throughout the text. Vector and tensor quantities are typically represented with boldface type, while scalars and individual components of vectors and tensors are written in italics. The index notation is often used for clarity, following the Einstein summation convention and

distinguishing between covariant (subscript) and contravariant (superscript) components. Current configuration indices are written in lower case Latin, reference configuration indices in upper case Latin, and intermediate configuration indices are written using Greek symbols. Capitalized symbols generally denote homogenized quantities and lower-case symbols, for the most part, denote local values. Quantities corresponding specifically to a stress-free state are often distinguished with a tilde above. Juxtaposition implies summation over two repeated adjacent indices (e.g., $(\mathbf{AB})_a^{\cdot b} = A_{ac}B^{cb}$). The dot (scalar) product of vectors is represented by the symbol "$\cdot$" (e.g., $\mathbf{a}\cdot\mathbf{b} = a^a g_{ab} b^b$, with g_{ab} components of the metric tensor). The symbol "$\otimes$" represents the tensor (outer) product (e.g., $(\mathbf{a}\otimes\mathbf{b})^{ab} = a^a b^b$). Additional notation is clarified as needed later in the text.

2. Multiscale coordinates

We consider a statistical volume element (SVE) of crystalline metal consisting of an arbitrary number of grains, whose representation in the current (deformed) configuration may also include damage entities such as explicit voids, cracks, and shear discontinuities. The SVE represents a continuum "point" in a macroscopic analysis. We label the aggregate an SVE (cf. Ostoja-Starzewski, 1998) rather than a representative volume element (RVE—cf. Hill, 1963; Hashin, 1964), since we do not assume a priori the statistical homogeneity of pertinent response functions, such as effective stiffness, for example. Mesoscopic (i.e., local) current and reference coordinates within the SVE are labeled $\mathbf{x}$ and $\mathbf{x}_0$, respectively, with the mesoscopic motion denoted by $\mathbf{x} = \boldsymbol{\varphi}(\mathbf{x}_0, t)$, and with time denoted by t. Similarly, macroscopic (i.e., global) current and reference coordinates for the SVE are labeled $\mathbf{X}$ and $\mathbf{X}_0$, respectively, with the macroscopic motion denoted by $\mathbf{X} = \boldsymbol{\Phi}(\mathbf{X}_0, t)$. The macroscopic coordinates describe the collective behavior of an aggregate of grains (O($\sim 10^{-4}$–10^{-3} m)) as manifested by SVE boundary motions, while the mesoscopic coordinates represent the local behavior of individual grains, sub-grains, inclusions, and damage entities within the aggregate (typically O($\sim 10^{-6}$–10^{-5} m)). Each SVE, while associated with a single material "point" $\mathbf{X}_0$ (macroscale), is considered to encompass a finite zone of surrounding material at a more refined scale of observation $\mathbf{x}_0$ (mesoscale). Fig. 1 depicts the motions, configurations, and corresponding coordinates, at the meso- and macroscales, for an SVE with material coordinates $\mathbf{X}_0$ and consisting of multiple grains and damage entities, all contained within a deforming structure.

Henceforward, as shown in Fig. 1, all tensorial quantities at both meso- and macroscales are referred to a coincident system of general curvilinear coordinates in each configuration; i.e., $x_0^A = X_0^A$ and $x^a = X^a$ $(A, a = 1, 2, 3)$. We assign a single set of both reference $(\mathbf{X}_0)$ and current $(\mathbf{X})$ coordinates to describe the mean motion of each SVE, while allowing variation in local coordinates $\mathbf{x}_0$ and $\mathbf{x}$ within the SVE. The covariant components of the metric tensor in the current configuration are labeled by $g_{ab} = \mathbf{g}_a \cdot \mathbf{g}_b$, with current basis vectors denoted by $\mathbf{g}_a$ and $\mathbf{g}_b$. Similarly, the covariant components of the metric tensor in the reference configuration satisfy $G_{AB} = \mathbf{G}_A \cdot \mathbf{G}_B$, with reference basis vectors labeled $\mathbf{G}_A$ and $\mathbf{G}_B$. We also use the notation $g \equiv \det \mathbf{g}$ and $G \equiv \det \mathbf{G}$ for the determinants of coordinate metric tensors. In what follows, we define macroscopic deformation tensors as volume averages of local, mesoscopic tensors defined at locations *within* the SVE (cf. Eq. (5)). It is essential that these local tensors be expressed with respect to a single set of *global* basis vectors and covectors in each relevant configuration, such that the volume averaging procedures are meaningful and accurate (Lippmann, 1996). This requirement also holds for volume averaging of tensor components associated with incompatible configurations, where anholonomic basis vectors are typically implied (e.g., Eq. (20)). Thus, basis vectors may change from point to point at the macroscopic level (i.e., with changes in $\mathbf{X}_0$ and $\mathbf{X}$, if general curvilinear coordinates are beneficial), but are restricted to be fixed—only when such volume averaging procedures are used—with respect to local coordinates $\mathbf{x}_0$ and $\mathbf{x}$ within each SVE, whose (global) centroidal coordinates are given by $\mathbf{X}_0$ and $\mathbf{X}$.

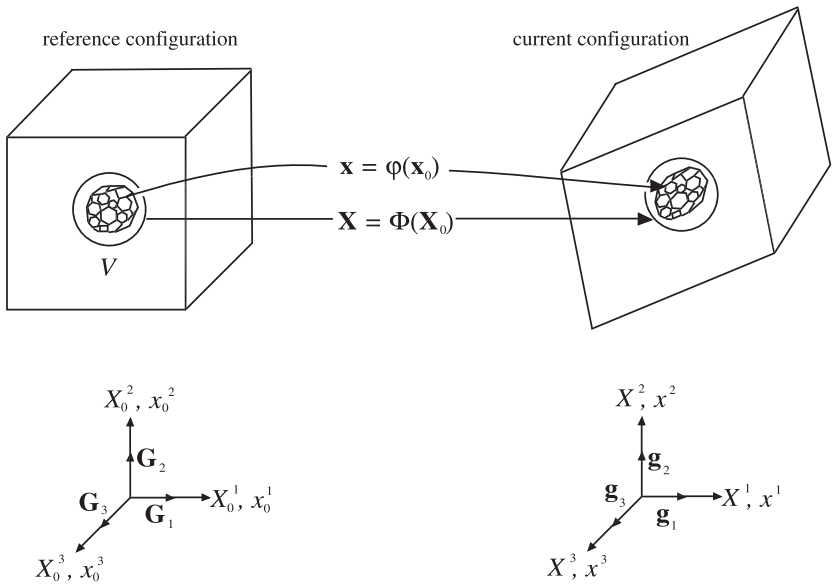

Fig. 1. Motions, configurations, and coordinates at the meso- and macroscales.

3. The macroscopic deformation gradient

The macroscopic deformation gradient $\mathbf{F}$, for the SVE centered at $\mathbf{X}_0$, is defined completely in terms of the motion of the external boundary of the SVE (cf. Hill, 1972), i.e.,

$$\mathbf{F} \equiv \frac{\partial \mathbf{\Phi}}{\partial \mathbf{X}_0} \equiv \frac{1}{V} \int_S \mathbf{x} \otimes \mathbf{n} \, \mathrm{d}S. \tag{1}$$

In Eq. $(1)_1$ we have tacitly assumed the compatibility of the total deformation gradient at the *macroscale*, i.e., $\partial F^a_{\cdot A}/\partial X^B_0 = \partial F^a_{\cdot B}/\partial X^A_0$. Also, V is the total scalar volume of the SVE in the reference state, while S is the external boundary surface of the SVE in the reference configuration, with corresponding unit outward normal covector $\mathbf{n}$. As indicated in Fig. 2, $\mathbf{F}$ depends only on the motion of the *external* boundary of the SVE and consists of the elastoplastic deformation of the crystalline matrix and the net contribution attributed to local damage entities (e.g., cracks, voids, and shear discontinuities) within the SVE. Also shown in Fig. 2, the state of the SVE in the reference (undeformed) configuration is labeled B_{ref}, and the state of the SVE in the current (deformed) configuration is labeled B_{cur}.

At the *mesoscale*, the local deformation is by definition incompatible when damage entities are introduced within the SVE. This means that current configuration coordinates $\mathbf{x}$ are not single-valued functions

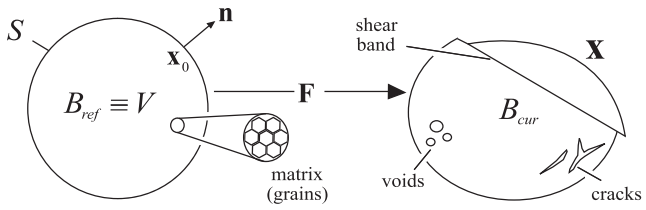

Fig. 2. Macroscopic deformation gradient for SVE.

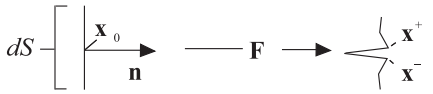

Fig. 3. Multi-valued boundary coordinates.

of $\mathbf{x}_0$ throughout the entire SVE: for example, such coordinates do not exist within the "empty spaces" between crack faces or inside voids. Eq. (1) is therefore *not* an invocation of the *classical* Gauss's theorem (cf. Malvern, 1969; Hill, 1972; Nemat-Nasser, 1999) when damage is present, since the body is no longer simply connected, and a local deformation gradient $\mathbf{f}$ does not exist throughout the entire SVE. However, we can still execute the calculation defined in Eq. (1) regardless of the simple-connectivity of the SVE, so long as current coordinates $\mathbf{x}$ are available over its outer boundary. For cases in which damage entities traverse the boundary, such that the current coordinates are multi-valued functions of the reference coordinates, we refer to the situation depicted in Fig. 3. A material point $\mathbf{x}_0$ along S—with normal covector (i.e., covariant vector) $\mathbf{n}$ and associated scalar differential area element $\mathrm{d}S$—is mapped during the course of the macroscopic deformation to two points $\mathbf{x}^+$ and $\mathbf{x}^-$ on opposing crack faces in the current configuration. The corresponding contribution to Eq. (1) is then defined simply as the average contribution of each local current configuration point, i.e., $(2V)^{-1}(\mathbf{x}^+ \otimes \mathbf{n}\,\mathrm{d}S + \mathbf{x}^- \otimes \mathbf{n}\,\mathrm{d}S)$. A similar procedure may be invoked when a shear band or void crosses the external boundary of the SVE.

Our restriction that the macroscopic deformation gradient $\mathbf{F}$ remains compatible precludes the modeling of macroscopic crack extension (e.g., cracks of sizes much larger than the SVE). Instead, we focus on distributed mesoscopic entities within the SVE, such that at the macrolevel, the material is regarded as a smooth continuum. This assumption will later permit specification of continuum-type relations (and traditional continuum finite elements in numerical simulations) to govern the evolution of polycrystalline material behavior in the spirit of previous macroscopic plasticity and damage models of Gurson (1977) and Bammann et al. (1993), for example. Henceforward, we shall use the terms "deformation", "deformation map", and "deformation gradient" interchangeably to denote any of the two-point tensors—including individual contributions from elasticity, plasticity, and damage—comprising the total deformation gradients at the meso- or macroscales, even though these tensors are generally incompatible (i.e., unlike $\mathbf{F}$ in Eq. (1) they are not true gradients of motion functions).

4. An additive–multiplicative decomposition

The total deformation gradient of Eq. (1) is now partitioned, in an additive fashion, into contributions from the matrix material (i.e., elastoplastic grains), $\mathbf{F}^{\mathrm{m}}$, and contributions from local damage incompatibilities (i.e., moving internal free surfaces or displacement discontinuities), $\mathbf{F}^{\mathrm{d}}$:

$$\underbrace{\mathbf{F}}_{\text{external surface of SVE}} = \underbrace{\mathbf{F}^{\mathrm{m}}}_{\text{bulk matrix grains}} + \underbrace{\mathbf{F}^{\mathrm{d}}}_{\text{internal surfaces (damage)}} . \tag{2}$$

As will be demonstrated later (Section 5), derived in rigorous detail in terms of the generalized Gauss's theorem in Appendix A, and discussed by Davison (1995), the additive decomposition (2) arises as a natural extension of the volume averaging process—using basic calculus arguments the surface integral (1) may be considered as the limit of a Riemann sum—and allows us to account for the contributions of individual damage entities in an explicit manner.

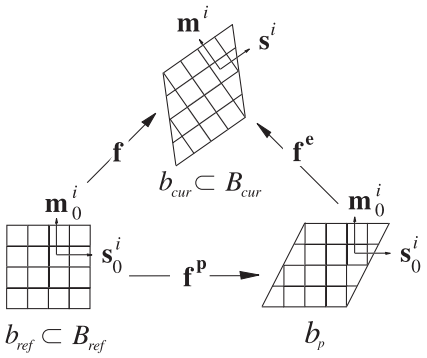

Fig. 4. Local configurations associated with multiplicative decomposition of the matrix deformation gradient at the mesoscale.

We now assume that the local deformation within undamaged regions of the matrix is describable via the multiplicative decomposition of classical crystal plasticity theory (cf. Rice, 1971; Teodosiu and Sidoroff, 1976; Asaro, 1983):

$$\mathbf{f} \equiv \left.\frac{\partial \boldsymbol{\varphi}}{\partial \mathbf{x}_0}\right|_{\text{matrix}} = \mathbf{f}^{\text{e}}\mathbf{f}^{\text{p}}, \tag{3}$$

with the local matrix deformation gradient $\mathbf{f}$ decomposed into an elastic part $\mathbf{f}^{\text{e}}$, the stretch of which is associated with the local stress, and a deviatoric plastic part $\mathbf{f}^{\text{p}}$, attributed to the past history of dislocation glide on individual slip systems. Fig. 4 shows the local configurations associated with the decomposition $(3)_2$. The *local* reference and current configurations in Fig. 4 are identified as sub-elements of their corresponding macroscopic configurations: $\mathrm{d}V \equiv b_{\text{ref}} \subset B_{\text{ref}}$ and $\mathrm{d}V_{\text{cur}} \equiv b_{\text{cur}} \subset B_{\text{cur}}$. An additional local stress-free configuration b_{p}, arising from the plastic deformation $\mathbf{f}^{\text{p}}$ and not necessarily corresponding to any global configuration, is also shown. We remark that Eq. (3) describes deformation only in regions of the SVE where the crystalline matrix remains intact (and the deformation remains compatible), since $\boldsymbol{\varphi}$ is not continuous or single-valued locally at damage entities. For the problem of intergranular fracture, for example, Eq. (3) will describe the local deformation gradient within grains, but will not apply for local volume sub-elements that span disjoint grain boundaries within the SVE.

The current configuration slip direction and slip plane normal vectors, labeled $\mathbf{s}^{\text{i}}$ and $\mathbf{m}^{\text{i}}$, respectively, in Fig. 4, are related to the reference slip vectors $\mathbf{s}_0^{\text{i}}$ and $\mathbf{m}_0^{\text{i}}$, as follows (Rashid and Nemat-Nasser, 1992):

$$\mathbf{s}^{\text{i}} = \mathbf{r}^{\text{e}}\mathbf{s}_0^{\text{i}}, \quad \mathbf{m}^{\text{i}} = \mathbf{r}^{\text{e}-*}\mathbf{m}_0^{\text{i}}, \tag{4}$$

where $\mathbf{r}^{\text{e}}$ is the proper orthogonal rotation tensor associated with the right polar decomposition of the elastic deformation, $\mathbf{f}^{\text{e}} = \mathbf{r}^{\text{e}}\mathbf{u}^{\text{e}}$. The $(\ )^*$ notation in (4) corresponds to the dual map of a mixed-variant two-point tensor (Stumpf and Hoppe, 1997) and is associated with a horizontal exchange of indices when the index notation is used. In general, the rate of lattice rotation includes the spin associated with elastic deformation and rigid body motion of the lattice; however, in Eq. (4) the deformation of the lattice vectors associated with the (typically small) elastic stretch $\mathbf{u}^{\text{e}}$ is neglected.

We define the homogenized matrix deformation gradient, $\mathbf{F}^{\text{m}}$, as a volume average of the local matrix deformation gradient given by Eq. (3):

$$\mathbf{F}^{\text{m}} \equiv \frac{1}{V}\int_{V_{\text{m}}} \mathbf{f}\,\mathrm{d}V_{\text{m}} = \frac{1}{V}\int_{V_{\text{m}}} \mathbf{f}^{\text{e}}\mathbf{f}^{\text{p}}\,\mathrm{d}V_{\text{m}}, \tag{5}$$

where it is understood that the integration takes place only over compatibly deformed reference volume V_{m} (i.e., the matrix) within the SVE. Notice from Eqs. (1)–(3) and (5) that $\mathbf{F} = V^{-1}\int_{\mathrm{matrix}} \mathbf{f}\,\mathrm{d}V = \mathbf{F}^{\mathrm{m}}$ only when damage is absent, i.e. when $\mathbf{F}^{\mathrm{d}} = \mathbf{0}$ and $V = V_{\mathrm{m}}$. In other words, the term $\mathbf{F}^{\mathrm{d}}$ is a representation of the failure of Gauss's theorem for defining the homogenized deformation gradient of the *matrix* strictly in terms of the motion of the *exterior* boundary, since it reflects the contributions of moving internal boundaries that destroy the simple-connectivity of SVE. We emphasize that the damage deformation term $\mathbf{F}^{\mathrm{d}}$ in the additive decomposition of the deformation gradient (Eq. (2)) does not represent a tangent map for push-forward and pull-back operations, cannot be used to define an intermediate "configuration", and does not necessarily satisfy $\det \mathbf{F}^{\mathrm{d}} > 0$. The same may be said of $\mathbf{F}^{\mathrm{m}}$ when $\mathbf{F}^{\mathrm{d}}$ is non-zero.

We consider here the contributions of two general kinds of damage entities to the damage deformation gradient $\mathbf{F}^{\mathrm{d}}$ of Eq. (2):

$$\mathbf{F}^{\mathrm{d}} = {}^{\mathrm{v}}\mathbf{F}^{\mathrm{d}} + {}^{\mathrm{s}}\mathbf{F}^{\mathrm{d}}, \tag{6}$$

with ${}^{\mathrm{v}}\mathbf{F}^{\mathrm{d}}$ the contribution of "volumetric" defects and ${}^{\mathrm{s}}\mathbf{F}^{\mathrm{d}}$ the contribution of "surface" defects. We distinguish volumetric defects, such as spherical or ellipsoidal voids, from surface defects, such as planar cracks or localized shear bands, by considering the surface area-to-volume ratio of each flaw. An initial flaw volume $V_{\mathrm{v}}^{(j)}$ is associated with each volumetric defect j. Defect volumes in the reference configuration are attributed, for example, to void-nucleating inclusions or initial porosity. The contribution of these entities, for which we may attribute a small, but appreciable, volume in the reference configuration, may be described via the following expression (cf. Hill, 1963, 1972):

$${}^{\mathrm{v}}\mathbf{F}^{\mathrm{d}} \equiv \frac{1}{V}\sum_{j}\int_{S_{\mathrm{v}}} \mathbf{x}\otimes\mathbf{n}_{\mathrm{v}}^{(j)}\,\mathrm{d}S_{\mathrm{v}}^{(j)}, \tag{7}$$

where we have applied summation over j volumetric defects within the SVE, each with unit surface normal covector $\mathbf{n}_{\mathrm{v}}^{(j)}$ and surface area element $\mathrm{d}S_{\mathrm{v}}^{(j)}$. Fig. 5(a) illustrates the relevant geometric quantities for the contribution of a single void. Note that a multiplicative decomposition including a term representing the macroscopic deformation gradient contribution from volumetric defects may be used to precisely represent purely *isotropic* expansion, simply by considering the relationship between the volume change and the Jacobian determinant of the deformation gradient (Bammann and Aifantis, 1989). Definition (7), however, permits *anisotropic* damage deformation, and its requirement of a "reference configuration flaw" is analogous to the requirement of a non-zero initial porosity value in the damage evolution equations of many existing macroscopic descriptions from the literature (e.g., Cocks and Ashby, 1980, 1982; Bammann et al., 1993; Khaleel et al., 2001; Mahnken, 2002). We remark that when Eq. (7) applies,

$$\Theta = V^{-1}\sum_{j}\det\left(\left(V_{\mathrm{v}}^{(j)}\right)^{-1}\int_{S_{\mathrm{v}}}\mathbf{x}\otimes\mathbf{n}_{\mathrm{v}}^{(j)}\,\mathrm{d}S_{\mathrm{v}}^{(j)}\right)V_{\mathrm{v}}^{(j)} = V^{-1}\sum_{j}V_{\mathrm{v}}^{(j)}$$

is a measure of the average porosity in the SVE in the current configuration (per unit reference volume), the value of which cannot be calculated directly from ${}^{\mathrm{v}}\mathbf{F}^{\mathrm{d}}$. Here $V_{\mathrm{v}}^{(j)}$ is the scalar volume enclosed by $S_{\mathrm{v}}^{(j)}$, the boundary surface of the jth damage entity.

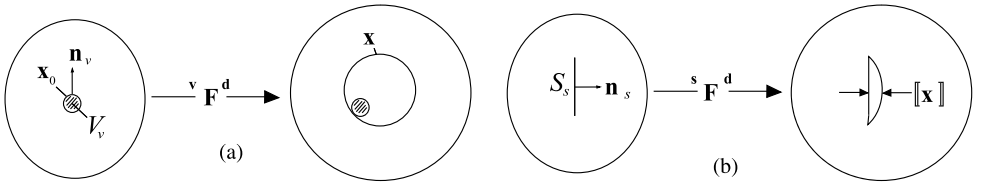

Fig. 5. Contribution to deformation gradient from (a) volumetric-type and (b) surface-type defects.

Consider now the contribution of internal surface-type defects, such as cracks and shear discontinuities. We use ${}^{\mathrm{s}}\mathbf{F}^{\mathrm{d}}$ to represent the macroscopic deformation attributed to such entities, which are of one spatial dimension less than that of the SVE (e.g., a 2D planar crack in a 3D volume). The local geometry of each defect k is described in terms of a displacement jump in the current configuration, written as $[\![\mathbf{x}]\!]$, a reference configuration surface $S_{\mathrm{s}}^{(k)}$—which could be a grain boundary plane prior to intergranular fracture, for example—and a corresponding reference configuration unit normal covector, $\mathbf{n}_{\mathrm{s}}^{(k)}$. Following Kachanov (1980), Davison (1995), Armero and Garikipati (1996), Pęcherski (1998), and Zhou and Zhai (1999), Eq. (7) reduces to the following for the contribution to the homogenized deformation gradient due to k surface-type defects:

$$ {}^{\mathrm{s}}\mathbf{F}^{\mathrm{d}} \equiv \frac{1}{V}\sum_{k}\int_{S_{\mathrm{s}}} [\![\mathbf{x}]\!] \otimes \mathbf{n}_{\mathrm{s}}^{(k)}\,\mathrm{d}S_{\mathrm{s}}^{(k)}. \tag{8} $$

Fig. 5(b) illustrates the geometric terms involved in definition (8) for a single crack. Note that in Cartesian coordinates the expression $\Theta = \mathrm{tr}({}^{\mathrm{s}}\mathbf{F}^{\mathrm{d}})$ yields the volume fraction of damage attributed to surface-type defects represented in this fashion (Kachanov, 1980).

Notice that while each part of Fig. 5 depicts a single damage entity (i.e., one void or one crack), multiple cracks and voids in combination are taken into account via superposition in Eqs. (6)–(8). Also, Eqs. (7) and (8) are fully applicable for describing voids and/or cracks of arbitrary shape, size, and connectivity, with the area integration taking place over the total ensemble of facets comprising damage entities (e.g., all void surfaces or crack branches).

We next introduce the two-point deformation tensor $\mathbf{F}^{\mathrm{e}}$ as the macroscopic "elastic" deformation mapping, generally not compatible with any prescribed coordinate field. We require that $\det \mathbf{F}^{\mathrm{e}} > 0$, permitting unique left and right polar decompositions, i.e. $\mathbf{F}^{\mathrm{e}} = \mathbf{V}^{\mathrm{e}}\mathbf{R}^{\mathrm{e}} = \mathbf{R}^{\mathrm{e}}\mathbf{U}^{\mathrm{e}}$, with $\mathbf{R}^{\mathrm{eT}} = \mathbf{R}^{\mathrm{e}-1}$, $\mathbf{V}^{\mathrm{eT}} = \mathbf{V}^{\mathrm{e}}$, and $\mathbf{U}^{\mathrm{eT}} = \mathbf{U}^{\mathrm{e}}$.

The elastic stretch tensors $\mathbf{V}^{\mathrm{e}}$ and $\mathbf{U}^{\mathrm{e}}$ are associated in the present model with the average macroscopic external stress, which we assume obeys the standard angular momentum balance in the current configuration (i.e., symmetric average Cauchy stress). The intermediate configuration $\widetilde{B}_{\mathrm{int}}$ of the SVE reached upon hypothetical instantaneous elastic unloading from the current configuration B_{cur} via the inverse of the elastic deformation gradient, $\mathbf{F}^{\mathrm{e}-1}$, corresponds to null traction conditions on the *external* boundary of the SVE (i.e., the traction $\tilde{\mathbf{t}} = \mathbf{0}$ along $\widetilde{S}$), as shown in Fig. 6. The left elastic stretch tensor $\mathbf{V}^{\mathrm{e}}$ is determined explicitly from

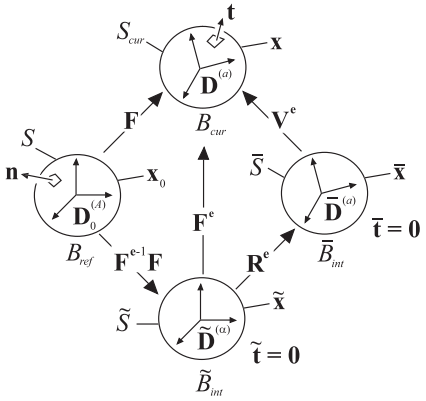

Fig. 6. Multiplicative decomposition of the macroscopic deformation gradient.

$$\mathbf{V}^{\mathrm{e}} = \left(\int_S \mathbf{x} \otimes \mathbf{n} \, \mathrm{d}S \right) \left(\int_S \bar{\mathbf{x}} \otimes \mathbf{n} \, \mathrm{d}S \right)^{-1}, \tag{9}$$

where $\bar{\mathbf{x}}$ are the local coordinates of the external boundary of the SVE corresponding to a second macroscopically stress-free intermediate configuration $\overline{B}_{\mathrm{int}}$, also shown in Fig. 6. Configuration $\overline{B}_{\mathrm{int}}$ arises from instantaneous removal of traction along the boundary of the SVE, constrained in such a way that the global rotation of the SVE, $\mathbf{R}^{\mathrm{e}-1}$, does not occur upon unloading. Specification of an intermediate unstressed configuration via *instantaneous* traction removal from the boundaries of the volume element was explicitly proposed by Kratochvil (1971), who remarked that viscous effects influence the designation of the unloaded configuration in rate-dependent solids. Rajagopal and Srinivasa (1998) also emphasized the dependence of unloaded state upon the rate of traction relaxation. Inertial effects are neglected by assumption during this idealized unloading procedure. Because we specify the response to traction removal to be instantaneous, any plastic deformation occurring upon unloading is idealized as rate independent. When $\bar{\mathbf{x}}$ are multi-valued functions of $\mathbf{x}_0$, a procedure analogous to that suggested for Eq. (1) is followed, accounting for contributions from $\bar{\mathbf{x}}$ on opposite sides of damage entities traversing $\overline{S}$ (cf. Fig. 3).

The orthogonal tensor $\mathbf{R}^{\mathrm{e}}$, which generally includes rigid body motion and elastic lattice rotation, is found from the solution of the integro-differential equation

$$\dot{\mathbf{R}}^{\mathrm{e}} \mathbf{R}^{\mathrm{eT}} = \boldsymbol{\Omega}^{\mathrm{e}} \equiv \frac{1}{V} \int_{V_{\mathrm{m}}} \boldsymbol{\omega}^{\mathrm{e}} \, \mathrm{d}V_{\mathrm{m}} = \frac{1}{V} \int_{V_{\mathrm{m}}} \dot{\mathbf{r}}^{\mathrm{e}} \mathbf{r}^{\mathrm{eT}} \, \mathrm{d}V_{\mathrm{m}}, \tag{10}$$

with initial conditions $\mathbf{R}^{\mathrm{e}}(t=0) = \mathbf{r}^{\mathrm{e}}(t=0) = \mathbf{1}$. In (10) the superposed dot denotes the material time derivative, and $\boldsymbol{\omega}^{\mathrm{e}}$ and $\boldsymbol{\Omega}^{\mathrm{e}}$ are, respectively, the mesoscopic and macroscopic lattice spin tensors referred to the current configuration. The local elastic lattice spin $\boldsymbol{\omega}^{\mathrm{e}}$ is dictated by the choice of constitutive model invoked for single crystals comprising the SVE (e.g., classical crystal plasticity theory). Mandel (1982) and Prantil et al. (1993) proposed analogous equations for the macroscopic *plastic* spin. We note that if the SVE is a single crystal with no heterogeneous internal deformation associated with grain subdivision or internal damage, then $\boldsymbol{\Omega}^{\mathrm{e}} = \boldsymbol{\omega}^{\mathrm{e}}$ and $\mathbf{R}^{\mathrm{e}} = \mathbf{r}^{\mathrm{e}}$. On the other hand, if the SVE contains a randomly oriented ensemble of grains whose net lattice vorticity satisfies $\boldsymbol{\Omega}^{\mathrm{e}} = \mathbf{0}$, the response exhibits isotropy in the sense of Kratochvil (1971).

Following Mandel (1973) and Naghdi and Srinivasa (1993), we assign to the SVE reference and current configuration triads of orthonormal director vectors, denoted $\mathbf{D}_0^{(A)}$ and $\mathbf{D}^{(a)}$ respectively, and satisfying

$$\mathbf{D}_0^{(A)} \cdot \mathbf{D}_0^{(B)} = \delta_B^A, \quad \mathbf{D}^{(a)} \cdot \mathbf{D}^{(b)} = \delta_b^a \qquad (A, a = 1, 2, 3), \tag{11}$$

where δ_B^A and δ_b^a are Kronecker delta symbols. We assume that the macroscopic elastic stretch is small, so that these directors rotate in a similar fashion to the slip directions of the constituent crystals (Eq. $(4)_1$), i.e.

$$\mathbf{D}^{(a)} = \delta_A^a \mathbf{R}^{\mathrm{e}} \mathbf{D}_0^{(A)}. \tag{12}$$

If we further stipulate that the director vectors remain stationary during the total irreversible deformation $\mathbf{F}^{\mathrm{e}-1}\mathbf{F}$, such that the intermediate configuration directors $\widetilde{\mathbf{D}}^{(\alpha)}$ satisfy $\widetilde{\mathbf{D}}^{(\alpha)} = \delta_A^\alpha \mathbf{D}_0^{(A)} = \delta_a^\alpha \mathbf{R}^{\mathrm{e}-1} \mathbf{D}^{(a)}$, our intermediate configuration $\widetilde{B}_{\mathrm{int}}$ is identified with Mandel's (1971, 1973) isoclinic configuration (Fig. 6). For the specific case of a homogeneously deforming single crystal, since $\mathbf{R}^{\mathrm{e}} = \mathbf{r}^{\mathrm{e}}$, the director vectors $\mathbf{D}^{(a)}$ rotate in an identical fashion to the slip plane normals and slip directions (Eq. (4)). In the general case of a heterogeneous polycrystal, the time-dependent rotation of the director vectors $\mathbf{D}^{(a)}$ is dictated by the volume-averaged spin of the lattice $\boldsymbol{\Omega}^{\mathrm{e}}$ defined by Eq. (10).

We now propose a multiplicative decomposition of the total deformation gradient:

$$\mathbf{F} = \mathbf{F}^{\mathrm{e}} \widetilde{\mathbf{F}} = \mathbf{F}^{\mathrm{e}} \left(\frac{1}{V} \int_S \tilde{\mathbf{x}} \otimes \mathbf{n} \, \mathrm{d}S \right), \tag{13}$$

with $\widetilde{\mathbf{F}} \equiv \mathbf{F}^{\mathrm{e}-1}\mathbf{F}$ the total residual deformation gradient between the reference configuration and the stress-free intermediate configuration, as is clear from Fig. 6. Local coordinates along the outer boundary $\widetilde{S}$ are denoted by $\tilde{\mathbf{x}}$. When damage entities intersect the boundary $\widetilde{S}$, rendering $\tilde{\mathbf{x}}$ multi-valued functions of $\mathbf{x}_0$, the contributions of $\tilde{\mathbf{x}}$ on opposite faces of damage entities are found using a procedure analogous to that employed for multi-valued coordinates $\mathbf{x}$ and $\bar{\mathbf{x}}$ in Eqs. (1) and (9), respectively. We note that the inverse elastic deformation $\mathbf{F}^{\mathrm{e}-1}$ includes any rearrangement of local damage entities upon the processes of macroscopic elastic unloading ($\mathbf{V}^{\mathrm{e}-1}$), including recovered deformation attributed to crack closure, if occurring. Likewise, $\widetilde{\mathbf{F}}$ includes the contributions of damage present in configuration $\widetilde{B}_{\mathrm{int}}$, in addition to contributions from non-recovered local elastoplasticity in the matrix grains (i.e., residual elastic lattice deformation and residual plastic deformation).

In the macroscopically unloaded intermediate configuration $\widetilde{B}_{\mathrm{int}}$, the local deformation gradient, $\tilde{\mathbf{f}}$, which is well-defined only within damage-free regions of matrix grains, is assumed to adhere to the following multiplicative decomposition:

$$\tilde{\mathbf{f}} \equiv \left.\frac{\partial \tilde{\mathbf{x}}}{\partial \mathbf{x}_0}\right|_{\mathrm{matrix}} = \tilde{\mathbf{f}}^{\mathrm{e}}\tilde{\mathbf{f}}^{\mathrm{p}}, \tag{14}$$

with $\tilde{\mathbf{x}}$ local coordinates within undamaged (i.e., compatibly deformed) regions of the SVE in configuration $\widetilde{B}_{\mathrm{int}}$, and with $\tilde{\mathbf{f}}^{\mathrm{e}}$ and $\tilde{\mathbf{f}}^{\mathrm{p}}$ the local residual elastic and plastic deformation gradients, respectively. We stress that the macroscopic configuration $\widetilde{B}_{\mathrm{int}}$ in Fig. 6 and the local intermediate configuration b_{p} of Fig. 4 generally do not coincide: local (residual) elastic deformation $\tilde{\mathbf{f}}^{\mathrm{e}}$ is present in the former, but absent in the latter. Furthermore, we emphasize that $\tilde{\mathbf{f}}$ is defined by the choice of stress-free intermediate configuration $\widetilde{B}_{\mathrm{int}}$, as uniquely specified by Eqs. (9) and (10).

Eq. (13) may be expanded into residual matrix deformation ($\widetilde{\mathbf{F}}^{\mathrm{m}}$) and residual damage ($\widetilde{\mathbf{F}}^{\mathrm{d}}$) contributions similarly to Eq. (2), i.e.,

$$\mathbf{F} = \mathbf{F}^{\mathrm{e}}(\widetilde{\mathbf{F}}^{\mathrm{m}} + \widetilde{\mathbf{F}}^{\mathrm{d}}), \qquad \widetilde{\mathbf{F}}^{\mathrm{m}} \equiv \mathbf{F}^{\mathrm{e}-1}\mathbf{F}^{\mathrm{m}}, \qquad \widetilde{\mathbf{F}}^{\mathrm{d}} \equiv \mathbf{F}^{\mathrm{e}-1}\mathbf{F}^{\mathrm{d}}. \tag{15}$$

An additive decomposition of the residual damage deformation gradient with volumetric and surface terms analogous to those comprising the total damage deformation gradient in Eq. (6) also applies. In such a description we replace $\mathbf{x}$ and $[\![\mathbf{x}]\!]$ in Eqs. (7) and (8) with pull-backs to the intermediate configuration, defined by $\tilde{\mathbf{x}}' \equiv \mathbf{F}^{\mathrm{e}-1}\mathbf{x}$ and $[\![\tilde{\mathbf{x}}']\!] \equiv \mathbf{F}^{\mathrm{e}-1}[\![\mathbf{x}]\!]$, respectively. We then have

$$\widetilde{\mathbf{F}}^{\mathrm{d}} = {}^{\mathrm{v}}\widetilde{\mathbf{F}}^{\mathrm{d}} + {}^{\mathrm{s}}\widetilde{\mathbf{F}}^{\mathrm{d}}, \tag{16}$$

$${}^{\mathrm{v}}\widetilde{\mathbf{F}}^{\mathrm{d}} \equiv \mathbf{F}^{\mathrm{e}-1}({}^{\mathrm{v}}\mathbf{F}^{\mathrm{d}}) = \frac{1}{V}\sum_{j}\int_{S_{\mathrm{v}}} \tilde{\mathbf{x}}' \otimes \mathbf{n}_{\mathrm{v}}^{(j)}\,\mathrm{d}S_{\mathrm{v}}^{(j)}, \tag{17}$$

$${}^{\mathrm{s}}\widetilde{\mathbf{F}}^{\mathrm{d}} = \mathbf{F}^{\mathrm{e}-1}({}^{\mathrm{s}}\mathbf{F}^{\mathrm{d}}) = \frac{1}{V}\sum_{k}\int_{S_{\mathrm{s}}} [\![\tilde{\mathbf{x}}']\!] \otimes \mathbf{n}_{\mathrm{s}}^{(k)}\,\mathrm{d}S_{\mathrm{s}}^{(k)}. \tag{18}$$

We remark that $\tilde{\mathbf{x}}'$ in Eqs. (17) and (18) *do not* necessarily represent the actual coordinates of the damage entities in configuration $\widetilde{B}_{\mathrm{int}}$, but instead give the coordinates of the current configuration damage entities pulled back to $\widetilde{B}_{\mathrm{int}}$ by the mesoscopically uniform elastic deformation $\mathbf{F}^{\mathrm{e}}$, in order to satisfy Eq. $(15)_3$ unconditionally. In fact, since a non-vanishing $\mathbf{F}^{\mathrm{d}}$ (damage in the current configuration) will generally lead to a non-vanishing $\widetilde{\mathbf{F}}^{\mathrm{d}}$, the latter deformation map will not vanish even if all damage entities physically close upon macroscopic unloading. This is because $\mathbf{F}^{\mathrm{e}}$ generally consists of both elastic matrix and (recoverable) damage deformations. However, for the special case of purely *irrecoverable* damage, and upon assuming that the macroscopic elastic stretch is negligible such that $\mathbf{F}^{\mathrm{e}} = \mathbf{R}^{\mathrm{e}}$, Eqs. (17) and (18) *do* give the actual geometry of the individual damage entities, rotated rigidly along with the SVE from B_{cur} to $\widetilde{B}_{\mathrm{int}}$ via $\mathbf{R}^{\mathrm{e}-1}$. By

"irrecoverable" damage we mean damage entities whose local geometrical characteristics (e.g., void size and shape, crack orientation and separation distance, etc.) do not change upon traction removal from the outer boundary of the SVE, a procedure embodied by the deformation map $\mathbf{V}^{e-1}$. By this definition, irrecoverable damage entities are identical geometrically in configurations B_{cur} and $\overline{B}_{int}$ of Fig. 6. Even when the macroscopic elastic stretch is neglected (i.e., $\mathbf{V}^e = \mathbf{1}$), the damage is not necessarily irrecoverable. On the other hand, for real elastoplastic materials, since during macroscopic unloading we would typically expect all damage entities to recover to some extent (e.g., some degree of crack closure upon elastic unloading), the notion of an irrecoverable damage entity is generally physically, but not mathematically, precluded when $\mathbf{V}^e \neq \mathbf{1}$. Also notice that we could have alternatively defined the residual damage deformation gradients of Eqs. (17) and (18) in terms of the actual geometries of damage entities in global configuration $\widetilde{B}_{int}$, at the same time adjusting our definitions for the current configuration damage deformations ${}^{v}\mathbf{F}^{d}$ and ${}^{s}\mathbf{F}^{d}$ in Eqs. (7) and (8) as push-forwards of ${}^{v}\widetilde{\mathbf{F}}^{d}$ and ${}^{s}\widetilde{\mathbf{F}}^{d}$, respectively, such that Eq. $(15)_3$ would be unconditionally satisfied.

The homogenized, residual deformation for the matrix, written as $\widetilde{\mathbf{F}}^{m}$, also adheres to

$$\widetilde{\mathbf{F}}^{m} = \mathbf{F}^{e-1}\left(\frac{1}{V}\int_{V_m} \mathbf{f}^{e}\mathbf{f}^{p}\,dV_m\right), \tag{19}$$

where we have invoked Eqs. (3), (13) and (15). In contrast to the plastic deformation gradient in the conventional macroscopic decomposition (cf. Lee and Liu, 1967; Lee, 1969), $\widetilde{\mathbf{F}}^{m}$ contains effects of local plastic deformation *and* local elastic deformation of the lattice, as well as contributions from any *recoverable* damage deformation embodied in $\mathbf{F}^{e-1}$. The homogenized residual plastic deformation $\overline{\mathbf{F}}^{p}$ is specified here as the solution of the integro-differential equation

$$\overline{\mathbf{L}}^{p} \equiv \dot{\overline{\mathbf{F}}}^{p}\overline{\mathbf{F}}^{p-1} \equiv \frac{1}{V}\int_{V_m} \dot{\mathbf{f}}^{p}\mathbf{f}^{p-1}\,dV_m, \tag{20}$$

i.e., the macroscopic plastic velocity gradient $\overline{\mathbf{L}}^{p}$ is defined as a volume average of the local plastic velocity gradient referred to local configuration b_p of Fig. 4.

A multiplicative decomposition for the total *matrix* deformation gradient is now proposed:

$$\mathbf{F}^{m} = \mathbf{F}^{e}\widetilde{\mathbf{F}}^{m} = \mathbf{F}^{e}\widetilde{\mathbf{F}}^{i}\overline{\mathbf{F}}^{p}. \tag{21}$$

Combining Eqs. (19) and (21) then results in the *meso-incompatibility deformation tensor* $\widetilde{\mathbf{F}}^{i}$, i.e.

$$\widetilde{\mathbf{F}}^{i} \equiv \widetilde{\mathbf{F}}^{m}\overline{\mathbf{F}}^{p-1} = \mathbf{F}^{e-1}\left(\int_{V_m} \mathbf{f}^{e}\mathbf{f}^{p}\,dV_m\right)\overline{\mathbf{F}}^{p-1}. \tag{22}$$

When Eqs. $(17)_2$ and $(18)_2$ represent the actual geometries of local damage entities within configuration $\widetilde{B}_{int}$—such as occurs when $\mathbf{F}^e = \mathbf{R}^e$ and the damage is completely irrecoverable, or if damage is absent ($\mathbf{F}^d = \mathbf{0}$)—the residual matrix deformation gradient can be written in terms of local residual elastic and plastic deformations:

$$\widetilde{\mathbf{F}}^{m} = \frac{1}{V}\int_{V_m} \tilde{\mathbf{f}}^{e}\tilde{\mathbf{f}}^{p}\,dV_m, \tag{23}$$

where we have used Eq. (14). In such special cases, the meso-incompatibility tensor takes the reduced form (see also Clayton and McDowell, 2003)

$$\widetilde{\mathbf{F}}^{i} = \left(\int_{V_m} \tilde{\mathbf{f}}^{e}\tilde{\mathbf{f}}^{p}\,dV_m\right)\overline{\mathbf{F}}^{p-1}. \tag{24}$$

From either Eq. (22) or Eq. (24) one may deduce that $\widetilde{\mathbf{F}}^{i}$ provides an indication of the heterogeneity of elastoplastic deformation within the matrix grains of the SVE. The $\widetilde{\mathbf{F}}^{i}$ tensor in Eq. (24) is in fact a kind of

weighted volume average of the residual elastic deformation term $\tilde{\mathbf{f}}^{\mathrm{e}}$, with the residual plastic deformation $\tilde{\mathbf{f}}^{\mathrm{p}}$ serving as the weighting multiplier. In the general case of heterogeneous residual elastic and plastic deformations within the SVE, $\widetilde{\mathbf{F}}^{\mathrm{i}}$ of Eq. (24) is a function of both elastic and plastic deformations. When considering the more general form given by Eq. (22), the effects of recoverable damage enter the $\widetilde{\mathbf{F}}^{\mathrm{i}}$ term through the macroscopic elastic deformation gradient $\mathbf{F}^{\mathrm{e}}$. Notice from Eq. (24) that $\widetilde{\mathbf{F}}^{\mathrm{i}} = \mathbf{1}$ when residual lattice deformation vanishes everywhere in the SVE and the plastic deformation is uniform throughout the time history of loading and unloading (i.e., when $\tilde{\mathbf{f}}^{\mathrm{e}} = \mathbf{1}$ and $\tilde{\mathbf{f}}^{\mathrm{p}} = \overline{\mathbf{F}}^{\mathrm{p}}$). Previous work regarding undamaged polycrystals (Clayton and McDowell, 2003) has demonstrated that the stretch associated with $\widetilde{\mathbf{F}}^{\mathrm{i}}$ is positively correlated with the distribution of local "incompatibility" at the mesoscale; i.e., the presence of local residual stresses and elastic lattice stretch (and commensurate elastic strain energy density) due to non-uniform elastoplastic deformation within the SVE in the intermediate configuration $\widetilde{B}_{\mathrm{int}}$. For this reason, we refer to the deformation term $\widetilde{\mathbf{F}}^{\mathrm{i}}$ as the "meso-incompatibility tensor". We comment that in the case of a homogeneously deforming, damage-free *single crystal*, we have $\mathbf{F} = \mathbf{f}$, $\mathbf{F}^{\mathrm{e}} = \mathbf{f}^{\mathrm{e}}$, $\widetilde{\mathbf{F}} = \widetilde{\mathbf{F}}^{\mathrm{m}} = \tilde{\mathbf{f}} = \tilde{\mathbf{f}}^{\mathrm{p}} = \mathbf{f}^{\mathrm{p}} = \overline{\mathbf{F}}^{\mathrm{p}}$, $\tilde{\mathbf{f}}^{\mathrm{e}} = \mathbf{1}$, $\widetilde{\mathbf{F}}^{\mathrm{d}} = \mathbf{F}^{\mathrm{d}} = \mathbf{0}$, and $\widetilde{\mathbf{F}}^{\mathrm{i}} = \mathbf{1}$, so the classical crystal plasticity decomposition of Rice (1971) and Asaro (1983) is recovered. In other words, $\mathbf{F} = \mathbf{F}^{\mathrm{e}}\overline{\mathbf{F}}^{\mathrm{p}} \rightarrow \mathbf{f} = \mathbf{f}^{\mathrm{e}}\mathbf{f}^{\mathrm{p}}$ when the SVE is a uniform undamaged single crystal. On the other hand, we emphasize that if the standard macroscopic decomposition $\mathbf{F} = \mathbf{F}^{\mathrm{e}}\mathbf{F}^{\mathrm{p}}$ is adopted with the assumption that $\mathbf{F}^{\mathrm{p}}$ is produced exclusively by homogenized dislocation motion (e.g., $\mathbf{F}^{\mathrm{p}} = \overline{\mathbf{F}}^{\mathrm{p}}$) at the SVE level for a damage-free *polycrystal*, local residual elastic stretch fields are tacitly neglected. Moreover, if the standard decomposition $\mathbf{F} = \mathbf{F}^{\mathrm{e}}\mathbf{F}^{\mathrm{p}}$ is invoked, with the volumetric part of $\mathbf{F}^{\mathrm{p}}$ representing the kinematics of damage (cf. Marin and McDowell, 1996, and references cited therein), anisotropic damage cannot be captured precisely—for example, shear bands or contacting sliding crack faces that induce no net volume change for the SVE.

Combining Eqs. (15) and (21) leads to an additive–multiplicative decomposition for the total deformation gradient:

$$\mathbf{F} = \mathbf{F}^{\mathrm{e}}(\widetilde{\mathbf{F}}^{\mathrm{i}}\overline{\mathbf{F}}^{\mathrm{p}} + \widetilde{\mathbf{F}}^{\mathrm{d}}). \tag{25}$$

In contrast to the above-mentioned two-term decomposition favored in the literature, Eq. (25) successfully represents residual elastic deformation of the lattice (embedded within $\widetilde{\mathbf{F}}^{\mathrm{i}}$) as well as anisotropic damage ($\widetilde{\mathbf{F}}^{\mathrm{d}}$). It should also be noted that while the kinematics of grain subdivision processes (see e.g., Butler and McDowell, 1998) are typically neglected by the usual two-term decomposition, these processes can be represented by our $\widetilde{\mathbf{F}}^{\mathrm{i}}$ tensor when the homogenization (i.e., volume averaging) methods are applied to a domain within a single crystal. Residual elastic deformation within a single crystal or polycrystal is often associated with scalar- or tensor-valued measures of dislocation density (Kröner, 1960, 2001), and our decomposition (25), while not applied in the current work towards resolving the fine-scale kinematics of the motion of discrete dislocations, is fully compatible with such descriptions of defect fields and can easily be projected to more refined length scales so long as the bulk material behaves as a continuum. The following section further elaborates upon the decompositions given in Eqs. (2) and (25).

5. Remarks on the additive and additive–multiplicative decompositions

We now present our motivation for using an additive form of the deformation gradient to describe damage. Notice from Eq. (25) that we *do not* advocate an additive decomposition for the elastic and inelastic terms or the displacement or velocity vectors (cf. Zbib, 1993; Shen, 1998; Voyiadjis and Park, 1999); such approaches, while perhaps mathematically acceptable, have been routinely criticized in the literature on physical grounds (cf. Lee, 1981). Instead, our additive decomposition applies solely to damage, and is a direct result of the volume averaging procedure and the connectivity properties of the SVE. We emphasize that our additive decomposition is an *exact result* stemming from the generalized Gauss's theorem, and is *not*

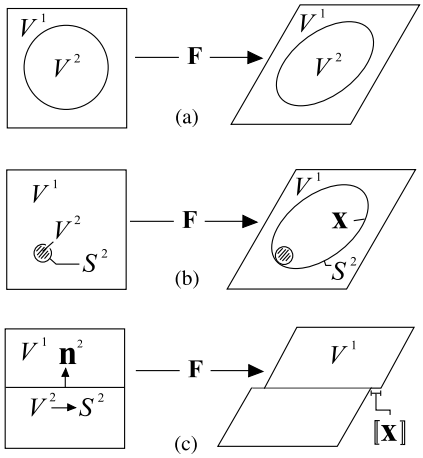

Fig. 7. Motivation for additive decomposition. Two-phase simply connected material (a), volumetric defect (b), and surface defect (c).

a constitutive assumption. Consider the two-dimensional deformation problem depicted in Fig. 7(a). The SVE consists of two parts: a circular volume (i.e., area with unit thickness) V^2 embedded in a square volume V^1. We assume that during the macroscopic deformation process symbolized by $\mathbf{F}$, the local deformation gradients $\mathbf{f}^1$ and $\mathbf{f}^2$ within each part are uniform, and that the body remains simply connected, such that Gauss's theorem applies. The volume-averaged deformation gradient then is found from Eq. $(1)_2$ as

$$\mathbf{F} \equiv \frac{1}{V}\int_S \mathbf{x}\otimes\mathbf{n}\,\mathrm{d}S = \frac{1}{V}\int_{V^1+V^2}\mathbf{f}\,\mathrm{d}V = \underbrace{\frac{1}{V}\int_{V^1}\mathbf{f}^1\,\mathrm{d}V^1}_{\mathbf{F}^1} + \underbrace{\frac{1}{V}\int_{V^2}\mathbf{f}^2\,\mathrm{d}V^2}_{\mathbf{F}^2} = \mathbf{F}^1+\mathbf{F}^2. \tag{26}$$

For the particular instance when the deformation gradients and volumes of the two parts are equal, we have $\mathbf{F}^1 = \mathbf{F}^2 = (1/2)\mathbf{F}$. Clearly, the quantities $\mathbf{F}^1$ and $\mathbf{F}^2$ do not individually represent tangent mappings of differential line elements, since for example in the instance of no deformation at all (i.e., $\mathbf{F} = \mathbf{1}$), each of these quantities is equal to half of the two-point identity map.

Now consider the case depicted in Fig. 7(b). In this situation, $V^2 \ll V^1$ is a rigid, void-nucleating inclusion surrounded by ductile matrix material V^1. The homogenized deformation gradient $\mathbf{F}$ for this case can be written as

$$\mathbf{F} = \frac{1}{V}\int_S \mathbf{x}\otimes\mathbf{n}\,\mathrm{d}S = \underbrace{\frac{1}{V}\int_{V^1}\mathbf{f}^1\,\mathrm{d}V^1}_{\mathbf{F}^{\mathrm{m}}} + \underbrace{\frac{1}{V}\int_{S^2}\mathbf{x}\otimes\mathbf{n}^2\,\mathrm{d}S^2}_{{}^{\mathrm{v}}\mathbf{F}^{\mathrm{d}}} = \mathbf{F}^{\mathrm{m}} + {}^{\mathrm{v}}\mathbf{F}^{\mathrm{d}}, \tag{27}$$

where, in essence, we have replaced the *deformed* volume of solid material V^2 of Fig. 7(a) with an equivalent volume of zero effective stiffness, the void surrounding the inclusion, in Fig. 7(b). Here $\mathbf{n}^2$ is the reference normal to surface S^2. Extending Eq. (27) to a distribution of j voids yields our definition for the volumetric damage deformation gradient given by Eq. (7). Now consider the situation depicted in Fig. 7(c), where the circle V^2 has degenerated into a one-dimensional surface S^2. In this case, the homogenized deformation gradient $\mathbf{F}$ is found as

$$\mathbf{F} = \frac{1}{V}\int_S \mathbf{x}\otimes\mathbf{n}\,\mathrm{d}S = \underbrace{\frac{1}{V}\int_{V^1}\mathbf{f}^1\,\mathrm{d}V^1}_{\mathbf{F}^{\mathrm{m}}} + \underbrace{\frac{1}{V}\int_{S^2}[\![\mathbf{x}]\!]\otimes\mathbf{n}\,\mathrm{d}S^2}_{{}^{\mathrm{s}}\mathbf{F}^{\mathrm{d}}}, \tag{28}$$

with $[\![\mathbf{x}]\!]$ the displacement discontinuity across the crack face in the current configuration. Summing over a field of k distributed microcracks provides our previous definition (8) for the damage deformation gradient arising from internal surface-type damage. The Appendix A of this paper contains more rigorous derivations of Eqs. (1), (2), and (6)–(8), among other relations, all following directly from application of the generalized Gauss's theorem.

One may stipulate that the since the void-nucleating inclusion (Fig. 7(b)) or the surface defect plane (Fig. 7(c)) exist in the reference configuration B_{ref}, this configuration is not a true, defect-free state for the material. To represent a completely damage-free reference polycrystal, we could easily include an additional preliminary deformation term $\boldsymbol{K}_0$ in the decomposition of Eq. (25), for example, such that

$$\boldsymbol{K} \equiv \mathbf{F}\boldsymbol{K}_0 = \mathbf{F}^{\mathrm{e}}(\widetilde{\mathbf{F}}^{\mathrm{i}}\overline{\mathbf{F}}^{\mathrm{p}} + \widetilde{\mathbf{F}}^{\mathrm{d}})\boldsymbol{K}_0, \tag{29}$$

where $\boldsymbol{K}$ is the total deformation gradient from the completely defect-free state (often called a "natural configuration" or "material manifold"—cf. Teodosiu, 1967, 1969; Maugin, 1993; Le and Stumpf, 1996) to the current configuration, and where $\boldsymbol{K}_0$ represents the insertion of defects within the configuration B_{ref} at time $t = 0$. However, for cases in which the initial volume fraction of defects (e.g., inclusions and voids) is small, and when all crack faces are closed at $t = 0$, the contribution to the total deformation gradient from the initial defect distribution is negligibly small and does not enter the kinematics, i.e. $\boldsymbol{K}_0 \approx \mathbf{1}$. Residual *elastoplasticity* present in initial configuration B_{ref} could also be included within $\boldsymbol{K}_0$ (cf. Teodosiu, 1967, 1969; Rice, 1971; Teodosiu and Sidoroff, 1976), but throughout the present work we assume the matrix in the reference configuration is a perfect lattice, free of dislocations and internal residual stress fields. In this framework, grain boundaries are idealized as discontinuities in initial lattice orientations between constituent crystals, rather than as dislocation aggregates with associated internal stress fields.

The additive–multiplicative decomposition given by Eq. (25) implies the existence of three macroscopic configurations for the SVE, as shown in Fig. 8. We recall in Fig. 8 the following notation. The *global* state of the entire SVE in the reference configuration is labeled B_{ref}; i.e., $B_{\text{ref}} \equiv V$. The state of the SVE in the current configuration is labeled B_{cur}, and the state of the SVE in the externally unloaded intermediate configuration is labeled $\widetilde{\boldsymbol{B}}_{\text{int}}$. *Local* configurations are labeled in a similar fashion; the local volume elements are enlarged in Fig. 8 for enhanced visibility of presentation. An individual local volume element in the reference state is labeled b_{ref}, such that $b_{\text{ref}} \equiv \mathrm{d}V \subset V \equiv B_{\text{ref}}$. Also depicted are the local configurations $\tilde{b}_{\text{int}} \subset \widetilde{\boldsymbol{B}}_{\text{int}}$ and $b_{\text{cur}} \subset B_{\text{cur}}$. Configuration b_{p} is identified with the stress-free intermediate configuration of

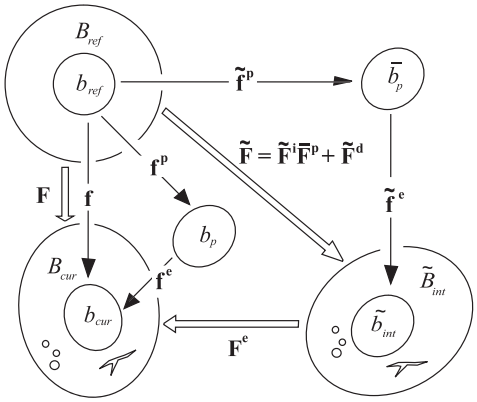

Fig. 8. Local and global configurations associated with the decomposition of the deformation gradient at multiple length scales.

crystal plasticity theory, as depicted previously in Fig. 4. The local stress-free configuration $\bar{b}_{\mathrm{p}}$, arising from the plastic deformation $\tilde{\mathbf{f}}^{\mathrm{p}}$ and not necessarily corresponding to any global configuration, is also shown.

Also, notice in Fig. 8 that the local stress-free intermediate configuration b_{p} and the local configuration $\tilde{b}_{\mathrm{int}}$ do not necessarily coincide unless the SVE is a homogeneously deformed single crystal, free of residual lattice stretch and rotation, and free of internal damage. Constituent local elements $\tilde{b}_{\mathrm{int}}$ may exhibit residual elastic stretch and residual stresses within globally unloaded configuration $\widetilde{B}_{\mathrm{int}}$. Such residual quantities are absent in the stress-free local configuration b_{p}. When the local residual elastic deformation fields vanish (e.g., inside a homogeneous damage-free single crystal) and when the unloading is purely elastic (no local plasticity upon load removal), the local configurations b_{p}, $\bar{b}_{\mathrm{p}}$ (due to residual plasticity, as shown in Fig. 8), and $\tilde{b}_{\mathrm{int}}$ coincide, meaning that $\widetilde{B}_{\mathrm{int}}$ is free of internal residual stresses. In such cases, $\widetilde{\mathbf{F}}^{\mathrm{i}} = \mathbf{1}$ and the plastic deformation field $\tilde{\mathbf{f}}^{\mathrm{p}} = \mathbf{f}^{\mathrm{p}} = \overline{\mathbf{F}}^{\mathrm{p}}$ is uniform throughout the SVE.

As a viable alternative to Eq. (25), an additive form for the *velocity gradient* could be used to model coupled elastoplasticity and damage, i.e.

$$\mathbf{L} \equiv \dot{\mathbf{F}}\mathbf{F}^{-1} = \mathbf{L}^{\mathrm{e}} + \mathbf{L}^{\mathrm{p}} + \mathbf{L}^{\mathrm{d}}, \tag{30}$$

where $\mathbf{L}^{\mathrm{e}}$, $\mathbf{L}^{\mathrm{p}}$, and $\mathbf{L}^{\mathrm{d}}$ represent the contributions of elasticity, plasticity (i.e., dislocation flux), and damage to the total spatial velocity gradient $\mathbf{L}$ (cf. Nemat-Nasser et al., 1981, who modeled the contributions of isotropic damage, and Pęcherski, 1998, who modeled microshear banding using an anisotropic $\mathbf{L}^{\mathrm{d}}$). However, we favor our deformation gradient decomposition over the rate decomposition in Eq. (30) for several reasons. Firstly, it is not clear to us how one should define explicitly the individual contributions of *all types* of flaws comprising a non-uniform distribution of damage entities (i.e., anisotropic damage) to the velocity gradient term $\mathbf{L}^{\mathrm{d}}$, in contrast to our ${}^{\mathrm{v}}\mathbf{F}^{\mathrm{d}}$ and ${}^{\mathrm{s}}\mathbf{F}^{\mathrm{d}}$ terms, whose definitions have been proposed and/or validated many times in the literature (cf. Hill, 1963, 1972, 1984; Kachanov, 1980; Davison, 1995; Armero and Garikipati, 1996; Pęcherski, 1998; Zhou and Zhai, 1999). Furthermore, determination of an evolution equation for $\mathbf{L}^{\mathrm{d}}$ using data from micromechanical (numerical) solutions and/or data from physical experiments would require accuracy-inhibiting numerical differentiation of the data, in contrast to measurement of deformation gradient terms, which requires no time differentiation. Finally, we remark that by defining a decomposition for the deformation gradient, such as in Eq. (25), one may determine the velocity gradient terms associated with elastoplasticity and damage by routine application of the material time derivative and chain rule for differentiation. In contrast, Eq. (30) is potentially less descriptive since it leaves the decomposition of the total deformation gradient unresolved.

To summarize various physical phenomena captured by the macroscopic decomposition given in Eq. (25), we list below in Eq. (31) several "degenerate" cases and the corresponding reduced forms of Eq. (25):

$$\begin{aligned}
&\text{general form}: \quad \mathbf{F} = \mathbf{F}^{\mathrm{e}}(\widetilde{\mathbf{F}}^{\mathrm{i}}\overline{\mathbf{F}}^{\mathrm{p}} + \widetilde{\mathbf{F}}^{\mathrm{d}}),\\
&\text{elasticity}: \quad \widetilde{\mathbf{F}}^{\mathrm{i}} = \overline{\mathbf{F}}^{\mathrm{p}} = \mathbf{1},\ \widetilde{\mathbf{F}}^{\mathrm{d}} = \mathbf{0} \rightarrow \mathbf{F} = \mathbf{F}^{\mathrm{e}},\\
&\text{homogeneous single crystal plasticity}: \quad \widetilde{\mathbf{F}}^{\mathrm{i}} = \mathbf{1},\ \widetilde{\mathbf{F}}^{\mathrm{d}} = \mathbf{0} \rightarrow \mathbf{F} = \mathbf{F}^{\mathrm{e}}\overline{\mathbf{F}}^{\mathrm{p}},\\
&\text{polycrystal plasticity}: \quad \widetilde{\mathbf{F}}^{\mathrm{d}} = \mathbf{0} \rightarrow \mathbf{F} = \mathbf{F}^{\mathrm{e}}\widetilde{\mathbf{F}}^{\mathrm{i}}\overline{\mathbf{F}}^{\mathrm{p}},\\
&\text{elasticity with damage}: \quad \overline{\mathbf{F}}^{\mathrm{p}} = \mathbf{1} \rightarrow \mathbf{F} = \mathbf{F}^{\mathrm{e}}(\widetilde{\mathbf{F}}^{\mathrm{i}} + \widetilde{\mathbf{F}}^{\mathrm{d}}).
\end{aligned} \tag{31}$$

We obviously have not listed all possibilities in Eq. (31) (e.g., rigid plasticity and all variations with damage). For the general case of heterogeneous polycrystalline elastoplasticity with damage, the full decomposition of Eq. (25) applies.

6. Conclusions

A combined additive–multiplicative decomposition of the macroscopic deformation gradient for an aggregate of crystalline grains has been proposed. The matrix deformation gradient is decomposed multiplicatively into terms representing recoverable elastic deformation, homogenized plastic deformation, and the meso-incompatibility deformation. The damage deformation gradient, unrestricted in terms of representation of anisotropy, consists of the summed contributions of individual entities (e.g., cracks or voids) to the total deformation gradient measured in terms of the external boundary motion of the macroscopic volume element (SVE). The framework is particularly appealing to interaction with micromechanics treatments for various deformation and damage phenomena, including coupled anisotropic plasticity and damage. Future work will deal with multiscale balance laws and evolution equations to accompany the kinematic framework developed herein, with particular constitutive assumptions justified by experimental and/or numerical data.

Acknowledgements

We thank Dr. D.J. Bammann of Sandia National Laboratories (Livermore, CA) for helpful discussion. The authors are grateful for the support of the Army Research Office (ARO Award DAAG559810213).

Appendix A

We present here derivations of Eqs. (1), (2), and (6)–(8), which rely primarily on the generalized Gauss's theorem. The generalized Gauss's theorem takes the form (Malvern, 1969)

$$\int_V \nabla * \mathbf{a}\,\mathrm{d}V = \int_s \mathbf{n} * \mathbf{a}\,\mathrm{d}S, \tag{A.1}$$

where $\mathbf{a}$ is a scalar, vector, or tensor of arbitrary rank that has continuous first partial derivatives with respect to local coordinates, ∇ is the gradient operator (i.e., covariant derivative with respect to the symmetric metric connection), and $\mathbf{n}$ is the outward unit normal covector to local surface element $\mathrm{d}S$. The surface S, which encloses volume V, is required to be piecewise smooth and exhibit a topological "outside" and "inside", such that $\mathbf{n}$ may be clearly assigned for the "outside" of each surface element $\mathrm{d}S$. The volume V must be simply connected for a single continuous boundary surface S to suffice—otherwise, (A.1) may be applied over a summation of disjoint surfaces completely enclosing a volume that is not simply connected. The $*$ operator represents a general product that exhibits the distributive property—examples include the scalar (dot) product, the cross product, and the tensor (outer) product. The familiar divergence theorem is obtained from Eq. (A.1) when $*$ is the dot product.

We first consider cases wherein the body (SVE) is simply connected, enclosed by a single continuous surface (Fig. 9(a)). To arrive at the form used for Eq. (1), we replace $\mathbf{a}$ with current configuration coordinate functions $\mathbf{x}$, and we select V as a volume in the reference configuration enclosed by surface S, with local outward normal $\mathbf{n}$. The $*$ operator is chosen to be the outer product $\otimes$, giving

$$\int_V (\nabla \otimes \mathbf{x})\,\mathrm{d}V = \int_S (\mathbf{n} \otimes \mathbf{x})\,\mathrm{d}S, \tag{A.2}$$

or in index notation

$$\int_V \frac{\partial}{\partial x_0^J}(x^i)\,\mathrm{d}V = \int_S n_J x^i\,\mathrm{d}S, \tag{A.3}$$

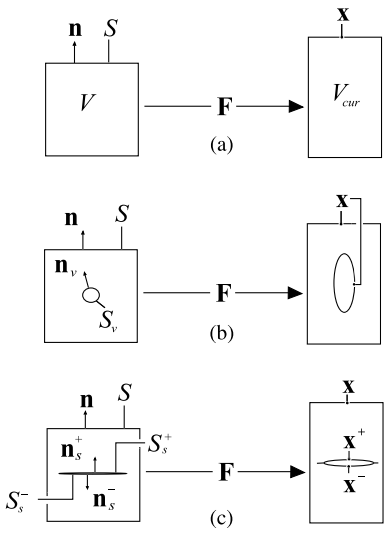

Fig. 9. Application of generalized Gauss's theorem: simply connected body (a), volumetric damage (b), and internal surface damage (c).

where we have assumed that covariant differentiation is equivalent to partial differentiation (i.e., a spatially constant reference metric tensor), true, for example, when the reference configuration is a Euclidean space, admitting Cartesian coordinates x_0^J. Further assuming that the local deformation gradient is *compatible* (i.e., integrable), i.e.,

$$\frac{\partial x^{\mathrm{i}}}{\partial x_0^J} = f^{\mathrm{i}}_J, \qquad x^{\mathrm{i}} = \varphi^{\mathrm{i}}(x_0^J, t), \tag{A.4}$$

substituting (A.4) into (A.3), transposing both sides, and dividing both sides by the total volume of the SVE in the reference configuration gives the homogenized deformation gradient $\mathbf{F}$ defined in Eq. (1), limited to the case of a damage-free (i.e., simply connected) SVE:

$$\mathbf{F} \equiv \frac{1}{V}\int_S \mathbf{x}\otimes\mathbf{n}\,\mathrm{d}S = \frac{1}{V}\int_V \mathbf{f}\,\mathrm{d}V = \frac{1}{V}\int_V \frac{\partial\boldsymbol{\varphi}}{\partial\mathbf{x}_0}\,\mathrm{d}V. \tag{A.5}$$

Now we consider cases when the body is no longer simply connected, corresponding to the evolution of damage in the form of internal volumetric defects (voids) and/or surface-type displacement discontinuities (cracks, shear bands). The situation where the body contains a single volumetric defect is shown in Fig. 9(b), and is considered first. In the reference configuration, the *external* boundary of the SVE is again labeled S, with outward unit normal covector $\mathbf{n}$, while the internal boundary corresponding to the volumetric defect is labeled S_{v}, with outward unit normal covector $\mathbf{n}_{\mathrm{v}}$. The homogenized deformation in the *matrix* then takes the form

$$\mathbf{F}^{\mathrm{m}} \equiv \frac{1}{V}\int_{V_{\mathrm{m}}} \mathbf{f}\,\mathrm{d}V_{\mathrm{m}} = \frac{1}{V}\int_S \mathbf{x}\otimes\mathbf{n}\,\mathrm{d}S + \frac{1}{V}\int_{S_{\mathrm{v}}} \mathbf{x}\otimes(-\mathbf{n}_{\mathrm{v}})\,\mathrm{d}S_{\mathrm{v}}, \tag{A.6}$$

taking into account the opposite orientation of the outward normal of the volumetric defect ($\mathbf{n}_{\mathrm{v}}$) with respect to the outward normal to the internal surface of the matrix material ($-\mathbf{n}_{\mathrm{v}}$). In (A.6), the local deformation gradient $\mathbf{f}$ is well-defined only within the referential matrix volume V_{m}, and not within the (empty space of) the defect. However, spatial coordinates $\mathbf{x}$ are available along the image of internal boundary S_{v} in the current configuration. If we then define

$$ {}^{\mathrm{v}}\mathbf{F}^{\mathrm{d}} \equiv \frac{1}{V}\int_{S_{\mathrm{v}}} \mathbf{x}\otimes\mathbf{n}_{\mathrm{v}}\,\mathrm{d}S_{\mathrm{v}}, \tag{A.7} $$

we may write

$$ \mathbf{F} \equiv \frac{1}{V}\int_{S} \mathbf{x}\otimes\mathbf{n}\,\mathrm{d}S = \underbrace{\frac{1}{V}\left(\int_{S}\mathbf{x}\otimes\mathbf{n}\,\mathrm{d}S - \int_{S_{\mathrm{v}}}\mathbf{x}\otimes\mathbf{n}_{\mathrm{v}}\,\mathrm{d}S_{\mathrm{v}}\right)}_{\mathbf{F}^{\mathrm{m}}} + \underbrace{\frac{1}{V}\int_{S_{\mathrm{v}}}\mathbf{x}\otimes\mathbf{n}_{\mathrm{v}}\,\mathrm{d}S_{\mathrm{v}}}_{{}^{\mathrm{v}}\mathbf{F}^{\mathrm{d}}}, \tag{A.8} $$

giving the net contribution of matrix deformation $\mathbf{F}^{\mathrm{m}}$ and a single volumetric defect ${}^{\mathrm{v}}\mathbf{F}^{\mathrm{d}}$ to the total deformation gradient $\mathbf{F}$. Summation with (A.7) over a distribution of j internal volumetric defects then gives our previous definition (Eq. (7)) for ${}^{\mathrm{v}}\mathbf{F}^{\mathrm{d}}$.

Now consider the situation of Fig. 9(c), wherein the referential internal defect is of one spatial dimension less than the dimension of the body (e.g., a 2D planar crack in a 3D body, or a line crack in a 2D body as shown). We divide the defect surface S_{s} in into two opposite faces: reference configuration (positive) surface S_{s}^{+} with corresponding outward unit normal covector $\mathbf{n}_{\mathrm{s}}^{+}$, and reference configuration (negative) surface S_{s}^{-} with corresponding outward unit normal covector $\mathbf{n}_{\mathrm{s}}^{-}$. The homogenized deformation gradient for the *matrix* then becomes

$$ \begin{aligned} \mathbf{F}^{\mathrm{m}} &\equiv \frac{1}{V}\int_{V_{\mathrm{m}}}\mathbf{f}\,\mathrm{d}V_{\mathrm{m}} = \frac{1}{V}\int_{S}\mathbf{x}\otimes\mathbf{n}\,\mathrm{d}S + \frac{1}{V}\int_{S_{\mathrm{s}}^{+}}\mathbf{x}^{+}\otimes(-\mathbf{n}_{\mathrm{s}}^{+})\,\mathrm{d}S_{\mathrm{s}}^{+} + \frac{1}{V}\int_{S_{\mathrm{s}}^{-}}\mathbf{x}^{-}\otimes(-\mathbf{n}_{\mathrm{s}}^{-})\,\mathrm{d}S_{\mathrm{s}}^{-} \\ &= \frac{1}{V}\int_{S}\mathbf{x}\otimes\mathbf{n}\,\mathrm{d}S - \frac{1}{V}\int_{S_{\mathrm{s}}^{+}}(\mathbf{x}^{+}-\mathbf{x}^{-})\otimes\mathbf{n}_{\mathrm{s}}^{+}\,\mathrm{d}S_{\mathrm{s}}^{+} = \frac{1}{V}\int_{S}\mathbf{x}\otimes\mathbf{n}\,\mathrm{d}S - \frac{1}{V}\int_{S_{\mathrm{s}}}[\![\mathbf{x}]\!]\otimes\mathbf{n}_{\mathrm{s}}\,\mathrm{d}S_{\mathrm{s}}, \end{aligned} \tag{A.9} $$

where we have used the relations $\mathbf{n}_{\mathrm{s}}\,\mathrm{d}S_{\mathrm{s}} \equiv \mathbf{n}_{\mathrm{s}}^{+}\,\mathrm{d}S_{\mathrm{s}}^{+} = -\mathbf{n}_{\mathrm{s}}^{-}\,\mathrm{d}S_{\mathrm{s}}^{-}$ and $[\![\mathbf{x}]\!] \equiv \mathbf{x}^{+}-\mathbf{x}^{-}$ for the referen ceconfiguration normal oriented surface elements and the current configuration coordinate jump associated with opposite faces of the surface defect. Here $\mathbf{x}^{+}$ and $\mathbf{x}^{-}$ are current configuration (spatial) coordinates along positive and negative crack faces. The damage deformation gradient associated with a single surface defect is then defined by

$$ {}^{\mathrm{s}}\mathbf{F}^{\mathrm{d}} \equiv \frac{1}{V}\int_{S_{\mathrm{s}}}[\![\mathbf{x}]\!]\otimes\mathbf{n}_{\mathrm{s}}\,\mathrm{d}S_{\mathrm{s}}, \tag{A.10} $$

from which

$$ \mathbf{F} \equiv \frac{1}{V}\int_{S}\mathbf{x}\otimes\mathbf{n}\,\mathrm{d}S = \underbrace{\frac{1}{V}\left(\int_{S}\mathbf{x}\otimes\mathbf{n}\,\mathrm{d}S - \int_{S_{\mathrm{s}}}[\![\mathbf{x}]\!]\otimes\mathbf{n}_{\mathrm{s}}\,\mathrm{d}S_{\mathrm{s}}\right)}_{\mathbf{F}^{\mathrm{m}}} + \underbrace{\frac{1}{V}\int_{S_{\mathrm{s}}}[\![\mathbf{x}]\!]\otimes\mathbf{n}_{\mathrm{s}}\,\mathrm{d}S_{\mathrm{s}}}_{{}^{\mathrm{s}}\mathbf{F}^{\mathrm{d}}}. \tag{A.11} $$

Summation over a distribution of k internal surface discontinuities then gives our previous definition (Eq. (8)) for ${}^{\mathrm{s}}\mathbf{F}^{\mathrm{d}}$. Superposition of Eqs. (A.7) and (A.10) for a single volumetric and a single surface defect, or Eqs. (7) and (8) for multiple volumetric and surface defects, gives the total damage deformation gradient (Eq. (6), repeated below):

$$ \mathbf{F}^{\mathrm{d}} = {}^{\mathrm{v}}\mathbf{F}^{\mathrm{d}} + {}^{\mathrm{s}}\mathbf{F}^{\mathrm{d}}. \tag{A.12} $$

The total deformation gradient $\mathbf{F}$ then has the form suggested originally in Eq. (2):

$$ \mathbf{F} = \mathbf{F}^{\mathrm{m}} + \mathbf{F}^{\mathrm{d}}, \tag{A.13} $$

where $\mathbf{F}^{\mathrm{m}}$ is defined by $(\mathrm{A.6})_1$ or, equivalently, $(\mathrm{A.9})_1$.

References

Armero, F., Garikipati, K., 1996. An analysis of strong discontinuities in multiplicative finite strain plasticity and their relation with the numerical simulation of strain localization in solids. Int. J. Solids Struct. 33, 2863–2885.

Asaro, R.J., 1983. Crystal plasticity. J. Appl. Mech. 50, 921–934.

Bammann, D.J., Aifantis, E.C., 1989. A damage model for ductile metals. Nucl. Eng. Des. 116, 355–362.

Bammann, D.J., Johnson, G.C., 1987. On the kinematics of finite-deformation plasticity. Acta Mech. 70, 1–13.

Bammann, D.J., Chiesa, M.L., Horstemeyer, M.F., Weingarten, L.I., 1993. Failure in ductile metals using finite element methods. In: Jones, N., Wierzbicki, T. (Eds.), Structural Crashworthiness and Failure. Elsevier, London, pp. 1–54.

Bilby, B.A., Gardner, L.R.T., Stroh, A.N., 1957. Continuous distributions of dislocations and the theory of plasticity. In: Extrait des Actes du IX^{e} Congrès International de Mécanique Appliquée, Brussels, pp. 35–44.

Brünig, M., 2002. Numerical analysis and elastic–plastic deformation behavior of anisotropically damaged solids. Int. J. Plast. 18, 1237–1270.

Butler, G.C., McDowell, D.L., 1998. Polycrystal constraint and grain subdivision. Int. J. Plast. 14, 703–717.

Clayton, J.D., McDowell, D.L., 2003. A multiscale multiplicative decomposition for elastoplasticity of polycrystals. Int. J. Plast. 19, 1401–1444.

Cocks, A.C.F., Ashby, M.F., 1980. Intergranular fracture during power-law creep under multiaxial stresses. Metal Sci. 14, 395–402.

Cocks, A.C.F., Ashby, M.F., 1982. Creep fracture by void growth. Prog. Mater. Sci. 27, 189–244.

Davison, L., 1995. Kinematics of finite elastoplastic deformation. Mech. Mat. 21, 73–88.

Duszek, M., Perzyna, P., 1991. The localization of plastic deformation in thermoplastic solids. Int. J. Solids Struct. 27, 1419–1443.

Fu, M.F., Saczuk, J., Stumpf, H., 1998. On fibre bundle approach to a damage analysis. Int. J. Eng. Sci. 36, 1741–1762.

Gurson, A.L., 1977. Continuum theory of ductile rupture by void nucleation and growth: part 1—yield criteria and flow rules for porous ductile media. J. Eng. Mat. Sci. Tech. 99, 2–15.

Hashin, Z., 1964. Theory of mechanical behaviour of heterogeneous media. Appl. Mech. Rev. 17, 1–9.

Hill, R., 1963. Elastic properties of reinforced solids: some theoretical principles. J. Mech. Phys. Solids 11, 357–372.

Hill, R., 1972. On constitutive macro-variables for heterogeneous solids at finite strain. Proc. R. Soc. Lond. A 326, 131–147.

Hill, R., 1984. On macroscopic effects of heterogeneity in elastoplastic media at finite strain. Math. Proc. Camb. Phil. Soc. 95, 481–494.

Kachanov, M., 1980. Continuum model of medium with cracks. J. Eng. Mech. 106, 1039–1051.

Khaleel, M.A., Zbib, H.M., Nyberg, E.A., 2001. Constitutive modeling of deformation and damage in superplastic materials. Int. J. Plast. 17, 277–296.

Kratochvil, J., 1971. Finite-strain theory of crystalline elastic-inelastic materials. J. Appl. Phys. 42, 1104–1108.

Kröner, E., 1960. Allgemeine kontinuumstheorie der versetzungen und eigenspannungen. Arch. Rat. Mech. Anal. 4, 273–334.

Kröner, E., 2001. Benefits and shortcomings of the continuous theory of dislocations. Int. J. Solids Struct. 38, 1115–1134.

Le, K.C., Stumpf, H., 1996. Nonlinear continuum theory of dislocations. Int. J. Eng. Sci. 34, 339–358.

Lee, E.H., 1969. Elastic–plastic deformation at finite strains. J. Appl. Mech. 36, 1–6.

Lee, E.H., 1981. Some comments on elastic–plastic analysis. Int. J. Solids Struct. 17, 859–872.

Lee, E.H., Liu, D.T., 1967. Elastic–plastic theory with application to plane-wave analysis. J. Appl. Phys. 38, 19–27.

Lippmann, H., 1996. Averaging or distributing stress and strain? Eur. J. Mech. A Solids 15, 749–759.

Mahnken, R., 2002. Theoretical, numerical and identification aspects of a new model class for ductile damage. Int. J. Plast. 18, 801–831.

Malvern, L.E., 1969. Introduction to the Mechanics of a Continuous Medium. Prentice-Hall, New Jersey.

Mandel, J., 1971. Plasticité Classique et Viscoplasticité. In: CISM Lecture Notes No. 97, Udine. Springer-Verlag, Wien.

Mandel, J., 1973. Equations constitutives et directeurs dans les milieux plastiques et viscoplastiques. Int. J. Solids Struct. 9, 725–740.

Mandel, J., 1982. Définition d'un repère privilégié pour l'etude des transformations an élastiques du polycrystal. J. Méc. Théo. Appl. 1, 7.

Marin, E.B., McDowell, D.L., 1996. Associative versus non-associative porous viscoplasticity based on internal state variable concepts. Int. J. Plast. 12, 629–669.

Maugin, G.A., 1993. Material Inhomogeneities in Elasticity. Chapman & Hall, London.

Maugin, G.A., 1994. Eshelby stress in elastoplasticity and ductile fracture. Int. J. Plast. 10, 393–408.

Murakami, S., 1983. Notion of continuum damage mechanics and its application to anisotropic creep damage theory. J. Eng. Mat. Tech. 105, 99–105.

Murakami, S., 1988. Mechanical modeling of material damage. J. Appl. Mech. 55, 280–286.

Murakami, S., 1990. A continuum mechanics theory of anisotropic damage. In: Boehler, J.P. (Ed.), Yielding, Damage, and Failure of Anisotropic Solids. London. pp. 465–482.

Naghdi, P.M., Srinivasa, A.R., 1993. A dynamic theory of structured solids. I. Basic developments. Phil. Trans. R. Soc. Lond. A 345, 425–458.

Nemat-Nasser, S., 1979. Decomposition of strain measures and their rates in finite deformation elastoplasticity. Int. J. Solids Struct. 15, 155–166.
Nemat-Nasser, S., 1999. Averaging theorems in finite deformation plasticity. Mech. Mat. 31, 493–523.
Nemat-Nasser, S., Li, Y.F., 1994. An algorithm for large-scale computational finite-deformation plasticity. Mech. Mat. 18, 231–264.
Nemat-Nasser, S., Mehrabadi, M.M., Iwakuma, T., 1981. On certain macroscopic and microscopic aspects of plastic flow in ductile materials. In: Nemat-Nasser, S. (Ed.), Three-dimensional Constitutive Relations and Ductile Fracture. North-Holland Publishing Company, pp. 157–172.
Ostoja-Starzewski, M., 1998. Random field models of heterogeneous materials. Int. J. Solids Struct. 35, 2429–2455.
Pantelides, S.T., 1994. First-principles mesoscopic dynamics in heterogeneous materials. J. Appl. Phys. 75, 3264–3272.
Park, T., Voyiadjis, G.Z., 1998. Kinematic description of damage. J. Appl. Mech. 65, 93–98.
Pęcherski, R.B., 1998. Macroscopic effects of micro-shear banding in plasticity of metals. Acta Mech. 131, 203–224.
Peirce, D., Asaro, R.J., Needleman, A., 1983. Material rate dependence and localization in crystalline solids. Acta. Metall. 31, 1951–1976.
Petryk, H., 1998. Macroscopic rate variables in solids undergoing phase transformations. J. Mech. Phys. Solids 46, 873–894.
Prantil, V.C., Jenkins, J.T., Dawson, P.R., 1993. An analysis of texture and plastic spin for planar polycrystals. J. Mech. Phys. Solids 41, 1357–1382.
Rajagopal, K.R., Srinivasa, A.R., 1998. Mechanics of the inelastic behavior of materials—part I, theoretical underpinnings. Int. J. Plast. 14, 945–967.
Rashid, M.M., Nemat-Nasser, S., 1992. A constitutive algorithm for rate dependent crystal plasticity. Comp. Meth. Appl. Mech. Eng. 94, 201–228.
Rice, J.R., 1971. Inelastic constitutive relations for solids: an internal-variable theory and its application to metal plasticity. J. Mech. Phys. Solids 19, 433–455.
Rice, J.R., 1976. The localization of plastic deformation. In: Koiter, W.T. (Ed.), Proc. 14th Int. Cong. Theo. Appl. Mech.. North-Holland, Amsterdam, pp. 207–220.
Rund, H., 1959. The Differential Geometry of Finsler Spaces. Springer, Berlin.
Saczuk, J., 2001. Continua with microstructure modelled by the geometry of higher-order contact. Int. J. Solids Struct. 38, 1019–1044.
Scheidler, M., Wright, T.W., 2001. A continuum framework for finite viscoplasticity. Int. J. Plast. 17, 1033–1085.
Shen, L., 1998. On the decomposition of deformation into elastic–plastic parts. J. Appl. Mech. 65, 1059–1061.
Steinmann, P., Carol, I., 1998. A framework for geometrically nonlinear continuum mechanics. Int. J. Eng. Sci. 36, 1793–1814.
Stumpf, H., Hoppe, U., 1997. The application of tensor algebra on manifolds to nonlinear continuum mechanics—invited survey article. Z. Agnew Math. Mech. 77, 327–339.
Stumpf, H., Saczuk, J., 2000. A generalized model of oriented continuum with defects. Z. Agnew. Math. Mech. 80, 147–169.
Stumpf, H., Saczuk, J., 2001. On a general concept for the analysis of crack growth and material damage. Int. J. Plast. 17, 991–1028.
Teodosiu, C., 1967. Contributions to the continuum theory of dislocations and initial stresses. I. Rev. Roum. Sci. Techn.—Méc. Appl. 12, 961–977.
Teodosiu, C., 1969. A dynamic theory of dislocations and its application to the theory of elastic–plastic continuum. In: Fundamental Aspects of Dislocation Theory. NBS Special Publication 317, US Government Printing Office, Gaithersburg, MD.
Teodosiu, C., Sidoroff, F., 1976. A finite theory of elastoplasticity of single crystals. Int. J. Eng. Sci. 14, 713–723.
Voyiadjis, G.Z., Park, T., 1999. The kinematics of damage for finite strain elasto-plastic solids. Int. J. Eng. Sci. 37, 803–830.
Zbib, H., 1993. On the mechanics of large inelastic deformations: kinematics and constitutive modeling. Acta Mech. 96, 119–138.
Zhou, M., Zhai, J., 1999. Modelling of micromechanical fracture using a cohesive finite element method. In: Furnish, M.D., Chhabildas, L.C., Hixson, R.S. (Eds.), Shock Compression of Condensed Matter—1999, Proc. of the Conf. of the American Physical Society Topical Group on Shock Compression of Condensed Matter, June 27–July 2, 1999. Snowbird, Utah, pp. 623–628.